Journal of Experimental Botany, Vol. 58, No. 4, pp. 797–806, 2007
Imaging Stress Responses in Plants Special Issue
doi:10.1093/jxb/erl208 Advance Access publication 30 November, 2006

Journal of Experimental Botany

SPECIAL ISSUE PAPER

Visualization of dynamics of plant–pathogen interaction by novel combination of chlorophyll fluorescence imaging and statistical analysis: differential effects of virulent and avirulent strains of *P. syringae* and of oxylipins on *A. thaliana*

Susanne Berger[1,*], Zuzana Benediktyová[2,3,*,†], Karel Matouš[2,3], Katharina Bonfig[1], Martin J. Mueller[1], Ladislav Nedbal[2,3] and Thomas Roitsch[1]

[1] *Julius-von-Sachs-Institute of Biosciences, Department of Pharmaceutical Biology, Julius-von-Sachs-Platz 2, D-97082 Würzburg, Germany*

[2] *Institute of Systems Biology and Ecology, Academy of Sciences of the Czech Republic*

[3] *Institute of Physical Biology, University of S. Bohemia, Zámek 136, 37333 Nové Hrady, Czech Republic*

Received 7 May 2006; Accepted 20 September 2006

Abstract

Pathogen infection leads to defence induction as well as to changes in carbohydrate metabolism of plants. Salicylic acid and oxylipins are involved in the induction of defence, but it is not known if these signalling molecules also mediate changes in carbohydrate metabolism. In this study, the effect of application of salicylic acid and the oxylipins 12-oxo-phytodienoic acid (OPDA) and jasmonic acid on photosynthesis was investigated by kinetic chlorophyll fluorescence imaging and compared with the effects of infection by virulent and avirulent strains of *Pseudomonas syringae*. Both pathogen strains and OPDA caused a similar change in fluorescence parameters of leaves of *Arabidopsis thaliana*. The response to OPDA appeared faster compared with that to the pathogens and persisted only for a short time. Infiltration with jasmonic acid or salicylic acid did not lead to a localized and distinct fluorescence response of the plant. To capture the faint early symptoms of the plant response, a novel algorithm was applied identifying the unique fluorescence signature—the set of images that, when combined, yield the highest contrast between control and infected leaf segments. Unlike conventional fluorescence parameters, this non-biased approach indeed detected the infection as early as 6 h after inoculation with bacteria. It was posssible to identify distinct fluorescence signatures characterizing the early and late phases of the infection. Fluorescence signatures of both infection phases were found in leaves infiltrated with OPDA.

Key words: Biotic stress, chlorophyll fluorescence, combinatorial fluorescence imaging, harmonically forced oscillations, jasmonic acid, OPDA, photosynthesis, salicylic acid.

Introduction

Defence mechanisms are aimed at preventing successful invasion and spreading of micro-organisms attacking the plant or to limit its detrimental effects. Besides non-host

* These authors contributed equally to this work.
† To whom correspondence should be addressed. E-mail: benedikty@greentech.cz

Abbreviations: F, chlorophyll fluorescence yield (subscripts 0, M, V, P, S define minimal, maximal, variable, peak, and steady-state level, whereas a prime indicates that the parameter was measured in light-exposed plant); F_V/F_M, maximum quantum yield of PSII photochemistry; $\Phi_P=F_V'/F_M'$, the efficiency of excitation energy capture by open PSII in the light-adapted state; $\Phi_N=1-\Phi_P=F_0'/F_M'$, quantum yield of non-photochemical processes in PSII in the light-adapted state; $\Phi_{PSII}=(F_M-F_S)/F_M$, quantum yield of PSII (non-cyclic) electron transport; $\Phi_{PSII}' = (F_M'-F_S')/F_M'$, effective quantum yield of PSII; $NPQ=F_M/F_M'-1$, non-photochemical chlorophyll fluorescence quenching; PSII, photosystem II; $Rfd=F_P/F_S-1$, chlorophyll fluorescence decrease ratio; $q_A=1-F_0'/F_M$, absolute quenching of ChlF; OPDA, 12-oxo-phytodienoic acid.

resistance against all races of a pathogen, host resistance confers resistance to specific, avirulent strains of a generally virulent pathogen. While the virulent strain is able to spread successfully in the host, the avirulent strain is recognized very early and the plant can effectively defend itself (Baker *et al*., 1997). One of the defence reactions typical for an incompatible interaction with an avirulent strain is programmed cell death of pathogen-attacked cells—the hypersensitive response (Heath, 2000). In addition, a whole plethora of defence responses such as the accumulation of phytoalexins, cell wall strengthening, and the expression of proteins with antimicrobial properties are induced (Dangl and Jones, 2001). The main difference in the plant responses to a virulent and an avirulent strain is the time-course and the extent of the defence reactions, which are much faster and stronger with the avirulent strain (Tao *et al*., 2003).

The induction of the defence responses is signalled by salicylic acid, ethylene, and jasmonic acid (Devoto and Turner, 2005). More recently, it was shown that 12-oxo-phytodienoic acid (OPDA), a biosynthetic precursor of jasmonic acid, is also biologically active (Stintzi *et al*., 2001; Taki *et al*., 2005). OPDA as well as jasmonic acid are derived from linolenic acid and are ubiquitous signals in the plant kingdom. Endogenous levels of these oxidized lipids increase after pathogen infection (Block *et al*., 2005). Exogenous application of these compounds induces defence gene expression (Creelman and Mullet, 1997). A strong support for an important role for these signalling molecules in defence against pathogens was provided by the altered susceptibility of mutants defective in oxylipin biosynthesis or signalling (Berger, 2002). The activities of OPDA only partly overlap with those of jasmonic acid, suggesting that OPDA has functions similar to jasmonic acid as well as an independent biological activity of its own. This is supported by the analysis of the mutants *dde2*, which is not able to synthesize OPDA and jasmonic acid, and *opr3*, which accumulates OPDA but not jasmonic acid. *dde2* but not *opr3* is more susceptible to necrotrophic fungi (Raacke *et al*., 2006). This indicates that OPDA is more important than jasmonic acid in the defence against these pathogens. In contrast, both mutants are more resistant to *Pseudomonas syringae*, suggesting that in the wild type, both jasmonic acid and OPDA negatively affect the defence against this pathogen. The salicylic acid pathway is the most important contributor to resistance against *P. syringae* (Delaney *et al*., 1994). A negative cross-talk between salicylic acid and oxylipins has been reported (Cui *et al*., 2005). Additionally, other research indicates that, depending on the concentration used, salicylic acid and jasmonic acid can have synergistic effects (Mur *et al*., 2006).

In addition to defence induction which is generally related to secondary metabolism, pathogen infection induces dramatic changes in the primary metabolism of the affected plant tissue. Several pathogens have been found to suppress photosynthesis of the host (Balachandran *et al*., 1994; Scholes and Rolfe, 1996; Scharte *et al*., 2005). In contrast, some pathogens pursue an alternative strategy maintaining photosynthesis of the host in green islands of the leaves (Angrasharma and Mandahar, 1993). With either of these pathogen strategies, the carbohydrate metabolism of the infected plant tissue is substantially modified. The sink strength of the plant is typically increased with assimilates mobilized for defence reactions (Roitsch *et al*., 2003; Roitsch and Gonzalez, 2004). Also affecting the plant metabolism, biotrophic pathogens drain the host resources by consuming assimilates. A co-ordinated regulation of defence, sink metabolism, and photosynthesis has been observed (Jang and Sheen, 1994; Herbers *et al*., 1996; Ehness *et al*., 1997), and sugars and defence-related stimuli were shown to mediate this regulatory mechanism independently (Ehness *et al*., 1997; Sinha *et al*., 2002). However, it is not clear whether carbohydrate metabolism and defence responses may also be differentially regulated. In favour of a co-ordinated regulation, jasmonic acid was shown to repress the expression of *RbcS* (Rubisco small subunit) transcriptionally and post-transcriptionally and to promote fruit ripening, senescence, and tuber formation (Creelman and Mullet, 1997).

The goal of the present study was to contribute to a better understanding of the regulation of photosynthesis in plants attacked by a pathogen. Fluorescence signatures in *Arabidopsis thaliana* responding to externally administered oxylipins and salicylic acid were being compared with signatures elicited by virulent and avirulent strains of the hemibiotrophic bacterium *P. syringae*. For this purpose, chlorophyll fluorescence imaging was used with a complex set of conventional (van Kooten and Snel, 1990; Maxwell and Johnson, 2000; Oxborough, 2004) and non-conventional (Nedbal and Brezina, 2002; Nedbal *et al*., 2003) actinic light protocols. Unique fluorescence signatures were identified by an advanced statistical analysis of the fluorescence image sequences. The technique resolved very early and late phases of the plant response to the pathogen infection as well as revealing differential effects of the signalling molecules.

Materials and methods

Plants

Wild-type *A. thaliana* Col *gl1* was grown with a 9 h light/15 h dark cycle in a controlled environment of a Sanyo Gallenkamp growth chamber (Leicester, UK). The plants were exposed to 150 μmol (photons) m^{-2} s^{-1} of white light at 25 °C and at 60% relative humidity during the day. During the night, the temperature was 20 °C and relative humidity 65%. Approximately 6-week-old plants with 10–12 fully developed leaves were used for the experiments.

Bacteria

The virulent bacterial strain *P. syringae* pv. *tomato* DC3000 was kindly provided by B Staskawicz, Berkley, CA, USA as well as the avirulent strain that differs by the plasmid carrying the *avrRpm1* gene. The bacteria were cultured in Kings B medium containing 50 mg l^{-1} rifampicin and additionally 10 mg l^{-1} tetracycline for the *avrRpm1* strain. An overnight culture was diluted 1:50 with fresh King's B medium prior to the experiment and cultivated for another 2 h at 28 °C. Bacterial cells were harvested by centrifugation (4 °C, 5000 rpm, 10 min) and dissolved first in 10 mM $MgCl_2$ to optical density (OD)=0.2 measured at 600 nm which corresponded to $\sim 10^8$ cfu ml^{-1}. The final cell concentration of 10^7 cfu ml^{-1} was achieved by another dilution. A needleless plastic syringe was used to gently press ~10 µl of bacterial suspension into the abaxial side of the leaf. The infiltration was done in the central part of one half of the leaf. The other half of the leaf remained untreated and served as a control. Control plants were inoculated with 10 mM $MgCl_2$. Four leaves of each plant were infiltrated and 2–5 plants were characterized for each of the treatments (virulent and avirulent *P. syringae*, OPDA, jasmonic acid, and salicylic acid).

Signalling molecules

For treatments with salicylic acid, a solution of the sodium salt obtained from Merck was used. Jasmonic acid was prepared by alkaline hydrolysis of jasmonic acid methyl ester. OPDA was synthesized from linolenic acid using linseed acetone powder and high-performance liquid chromatography (HPLC) purification as described in Parchmann *et al.* (1997). Oxylipins were diluted to a final concentration of 500 µM in 0.5% methanol before infiltration. Controls were infiltrated with 0.5% methanol, which did not result in effects on photosynthetic parameters at the time points indicated.

Kinetic imaging of chlorophyll fluorescence

Chlorophyll fluorescence imaging was performed with the FluorCam imaging fluorometer (P.S.I., Brno, Czech Republic, www.psi.cz) adapted to generate harmonically modulated actinic irradiance (Nedbal and Brezina, 2002). In order to evaluate contrast between the infected and healthy plant tissue, a complex actinic light protocol was employed that is described in detail in the Supplementary data available at *JXB* online). The protocol started with 10 min of dark adaptation followed by measuring flashes (620 nm) that yielded images of minimum fluorescence F_0 of the plant with a fully oxidized plastoquinone pool (F_0). A short saturating flash of 1200–1500 µmol (photons) m^{-2} s^{-1} of white light transiently reduced the plastoquinone pool, leading to an increase to the maximum fluorescence (F_M). After a short dark relaxation, the first actinic irradiance [50 µmol (photons) m^{-2} s^{-1}, 620 nm] was applied for 100 s and the corresponding transient of the Kautsky effect was recorded. Two saturating flashes [$F'_{M(1)}$ and $F'_{M(2)}$] were applied to probe the light-induced non-photochemical fluorescence quenching. The intensity of all saturating flashes applied in the protocol was kept between 1200 and 1500 µmol m^{-2} s^{-1} in the field of view. Fluorescence yield was also measured during 15 s of the dark adaptation followed by the actinic light period. Two other saturating flashes [$F'_{M(3)}$ and $F'_{M(4)}$] were applied to probe the relaxation of the non-photochemical fluorescence quenching. The experiment continued with 600 s of dark adaptation that was followed by an identical sequence of measuring events applied in the actinic light of 200 µmol (photons) m^{-2} s^{-1}. This actinic irradiance was chosen with respect to the capacity of the measuring instrument to represent the high light level.

The Kautsky transients with the two irradiance levels, I(t)=50 and 200 µmol m^{-2} s^{-1}, were followed by a battery of transients elicited by harmonically modulated irradiance $I(t)=I_0+I_0\cdot\sin(2\pi\cdot t/T)$, where T was the period of the harmonic forcing and $2I_0$ was the amplitude of the actinic light modulation. Details of the technique are described in Nedbal and Brezina (2002), and Nedbal *et al.* (2003, 2005). Here, fluorescence transients with forcing periods of T=1.5, 3, 6, 12, 24, and 48 s and with two amplitudes $2I_0$=80 and 160 µmol m^{-2} s^{-1} were included.

The *a priori* feature selection reduced the number of fluorescence images representing the entire fluorescence transient from 727 to 331: 247 in Kautsky effect transients and to 84=2×6×7 images in forced oscillations (Supplementary data available at *JXB* online). The seven images characterizing the forced oscillation for each period and amplitude of the forcing were the amplitudes and the phases of the fundamental component (period equal to forcing, T) and of two upper harmonics (one-half and one-third of the forcing period, T/2 and T/3), and average fluorescence yield.

These 331 images, each consisting of 512×512 pixels with 12 bit resolution, represented the basic data set characterizing the infection or infiltration response of a single plant. Typically, four attached mature leaves of each plant were treated and 2–5 plants were characterized in each of the treatment phases. Time points analysed were 3, 6, 9, 24, and 48 h after treatment. The selected leaves were gently placed on the black paper masks that hid other leaves and prevented substitution of treated and untreated leaves.

The statistical feature selection and the image segmentation were based on evaluating individual pixels, while individual leaves consisted of ~600 pixels.

Results

Effect of the infection of leaves by a virulent strain of P. syringae on conventional chlorophyll fluorescence parameters

A suspension of the virulent strain of *P. syringae* DC3000 was infiltrated into one of the two halves in each treated *A. thaliana* leaf. Four mature leaves of each plant were inoculated. Chlorophyll fluorescence transients of the entire plant were imaged before the inoculation, and 3, 6, 9, 24, and 48 h after the inoculation. Figure 1 shows leaf photographs and images of three selected conventional fluorescence parameters, F_V/F_M, Rfd, and NPQ, in control plants (left column) and in plants 6 h (middle column) and 24 h after the inoculation (right column). The white arrows indicate the infiltrated leaf segments. The false colour scales shown to the right of the fluorescence images indicate the amplitude of the particular parameter.

No symptoms were detectable by eye 6 h after the *P. syringae* infection, and only faint symptoms were visible after 24 h as documented by the colour photographs in the top row of Fig. 1. The F_V/F_M fluorescence parameter shown in the second row of Fig. 1 is interpreted as the maximum quantum yield of photosystem II (PSII) (Buffoni *et al.*, 1998; Genty *et al.*, 1989). It remained uniformly high, close to 0.8, 6 h after the inoculation (middle image). A localized decline of F_V/F_M was documented 24 h after the inoculation with bacteria. This was in agreement with an earlier report on a localized, infection-induced decrease in photosynthesis (Bonfig

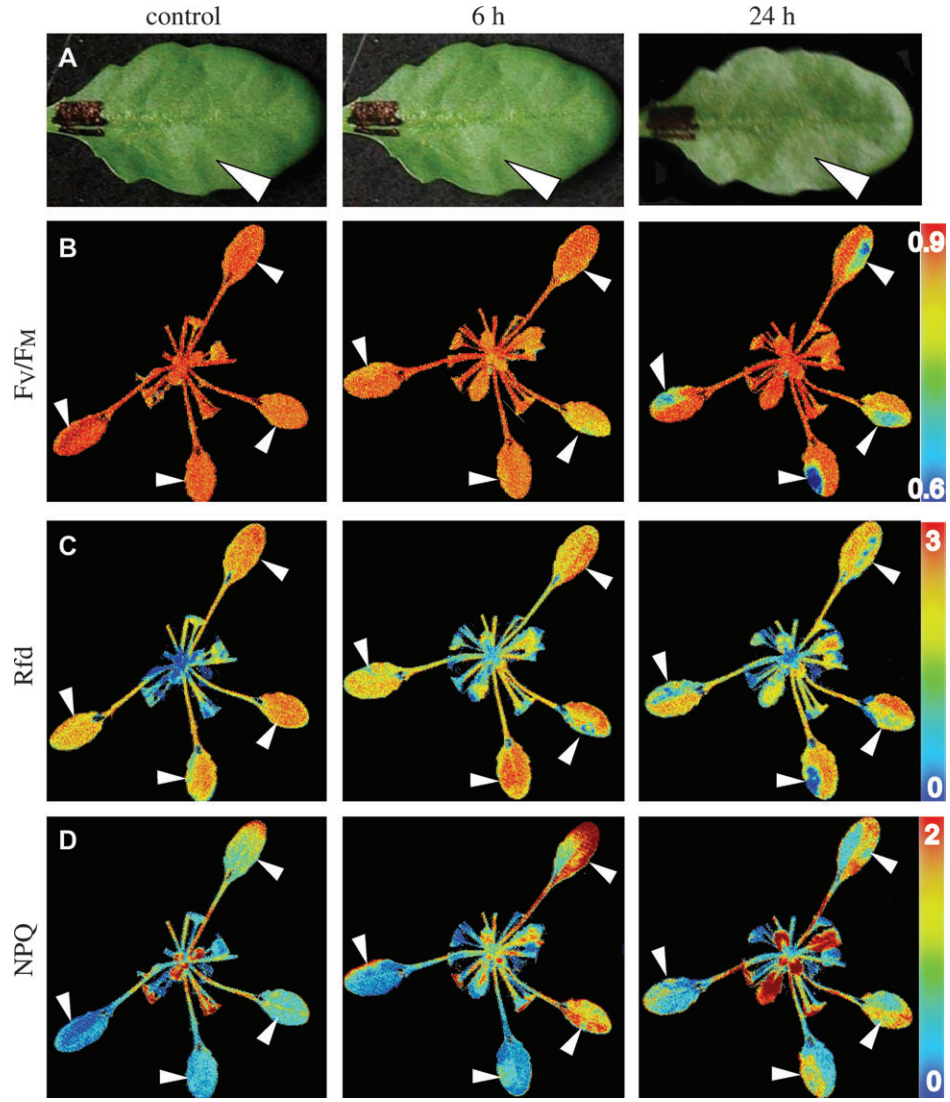

Fig. 1. *Arabidopsis thaliana* control plants (left column) and plants 6 h (middle column) and 24 h (right column) after infiltration by the virulent strain DC3000 of *P. syringae*. The control plants were untreated or infiltrated with 10 mM $MgCl_2$. The white arrows indicate which leaf and which half of the leaf was treated in the experiments. (A) Colour photographs. The leaves remained attached to plants. (B) False colour image showing F_V/F_M—maximum quantum yield of PSII. (C) Rfd—fluorescence decline ratio induced by 200 µmol (photons) m^{-2} s^{-1}. (D) NPQ—non-photochemical quenching induced by 200 µmol (photons) m^{-2} s^{-1}. The false colours show low values in blue and high values in red. The rainbow bar on the right of each image row shows the scaling.

et al., 2006). The third row in Fig. 1 documents pathogen-induced dynamics in another parameter that is interpreted as a measure of photosynthetic capacity, i.e. the fluorescence decrease ratio $Rfd=(F_P–F_S)/F_S$ (Lichtenthaler and Miehe, 1997; Lichtenthaler and Babani, 2000; Lichtenthaler *et al*., 2005*a*, *b*). In control plants, the Rfd parameter was significantly less uniform than F_V/F_M (first images from the left). The Rfd heterogeneity was further increased 6 h after the inoculation (middle image). The trend was not clear though, with a decrease of Rfd in the area of infection in half of the imaged leaves and with a faint increase in the remaining half (Fig. 1). The Rfd parameter was clearly depressed in the infected leaf segment 24 h after the inoculation with bacteria. The bottom row of the fluorescence images represents the dynamics of non-photochemical quenching, $NPQ=(F_M–F'_M)/F'_M$ (Horton and Ruban, 1992). An increase of NPQ in the area of infection was seen to various extents already after 6 h (middle image). Although the NPQ seemed to be more responsive to the infection than both F_V/F_M and Rfd at this time point, the reliability of this parameter was, however, reduced by its intrinsic leaf-to-leaf variability and by its sensitivity to the geometrical arrangement of the leaf with respect to the incident saturating light (patches in the control plant in Fig. 1). The other source of NPQ variability could be the intensity of the saturating flash that decreased towards the margins of the field of view from 1500 to 1200 µmol (photons) m^{-2} s^{-1}. The heterogeneity of the NPQ response

was further increased 24 h after the inoculation (right image). In some leaves, the NPQ was decreased in the core of the infected leaf area, whereas it was increased around it. This variability of NPQ lowers the potential of this parameter to serve as a reliable classifier of the infection.

Differential effects of oxylipin treatment and P. syringae *infection on chlorophyll fluorescence signatures*

Figure 1 shows that the infection differentially modified the three selected fluorescence parameters. Figure 2 shows the variability of the fluorescence response for a more extended set of conventional fluorescence parameters (Rohacek, 2002). The three spider plots show the dynamics of 19 conventional fluorescence parameters during the infection of *A. thaliana* by the virulent DC3000 (Fig. 2A) (Table S1 in the Supplementary data available at *JXB* online) and avirulent RPM1 (Fig. 2B) (Table S2 in the Supplementary data available at *JXB* online) strains of *P. syringae* and by infiltration with OPDA (Fig. 2C) (Table S3 in the Supplementary data available at *JXB* online). Each spider plot consists of three segments: the dark-shaded segment represents the parameters measured with dark-adapted plants, the light-shaded segment corresponds to the Kautsky induction measured in low light (50 µmol m^{-2} s^{-1}), and the segment without shading represents parameters measured in high actinic light (200 µmol m^{-2} s^{-1}). The distance from the centre of the spider plot indicates the relative change of the fluorescence parameter during the treatment. The change was measured by comparing the signals in the untreated half of the leaf with the leaf segment close to the application site. The values between the centre (–100%) and the solid black circle (0%) represent a decrease of the particular parameter during the infection. The values further to the perimeter (+200%) indicate an increase of the fluorescence parameter. Clearly, the OPDA infiltration elicited in 3 h a response (red line in Fig. 2C) that was similar to the fluorescence response observed in the plants infected by both strains of *P. syringae* 24 h after the infiltration (red line in Fig. 2A, B). The similarity of fluorescence changes of the three represented treatments indicates with a high confidence that their impact on photosynthetic processes is of a similar biological nature.

However, the time-course of the fluorescence changes was different with pathogens and with OPDA. The differences in the dynamics of the response to virulent and avirulent strains were small (compare the left and middle spider plots in Fig. 2). In line with expectations, the changes (green line) occurring 6 h after the infiltration were larger in certain parameters with the avirulent strain than with the virulent one. Yet, this faster onset of the response to the avirulent strain was not obvious any longer in plants 24 h after the inoculation (red line). In contrast to the infected plants, the symptoms rapidly disappeared in the OPDA-treated plants and were not observed 6 h after the infiltration (line not shown because of coincidence with the black line in Fig. 2C). The transient character of the OPDA-induced response can be caused by diffusion and dilution of the signalling compound in the plant tissue.

The changes of individual fluorescence parameters represented in the spider plots of Fig. 2 can be characterized approximately into three classes,

(i) The parameters measured in dark-adapted plants (F_0/F_M, F_V/F_M, and F_V/F_0). The conventional parameter F_V/F_M interpreted as the maximum quantum yield of PSII exhibited a small decline with all

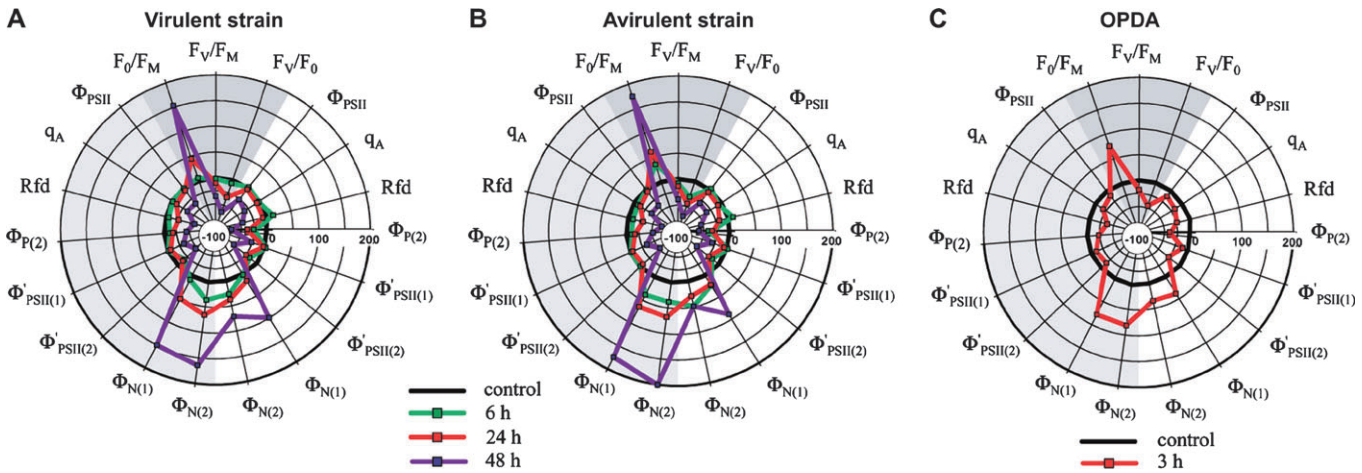

Fig. 2. Relative changes of mean values of selected fluorescence parameters in *A. thaliana* infected by the virulent strain (A) and by the avirulent *avrRPM1* strain (B) of *P. syringae*, and in plants infiltrated by the oxylipin signalling compound OPDA (C). The dark grey-shaded segments show parameters measured with dark-adapted plants. The fluorescence parameters measured during Kautsky induction and quenching analysis in low actinic light are shown in the lightly shaded segments. The non-shaded white segments show fluorescence parameters collected with high actinic light. The parameters collected with the harmonically modulated light are not shown.

treatments. The other mutually dependent parameters F_0/F_M and F_V/F_0 lack a clear physiological interpretation but were, in various forms, shown to yield a high contrast in revealing biotic and abiotic stresses (Nedbal *et al*., 2000; Soukupova *et al*., 2003). Also here, F_0/F_M dramatically increased and F_V/F_0 dramatically decreased during all the three treatments that are represented in Fig. 2.

(ii) The quantum yields of non-photochemical processes in PSII in light-adapted plants ($\Phi_N = F'_0/F'_M$) increased very significantly during the treatment regardless if measured during the first [$\Phi_{N(1)}$] or second of the saturating flashes [$\Phi_{N(2)}$]. The relative change was always higher in the low light (shaded background) than in the high light (no shading). The other fluorescence parameter, the NPQ [$NPQ=(F_M-F'_M)/F'_M$] is shown in Fig. 1 and discussed in the previous section.

(iii) The other parameters shown in Fig. 2 stagnated or decreased upon the treatment. The parameters $\Phi_{P(2)}$, $\Phi'_{PSII(2)}$ decreased more during induction in high light (unshaded sectors of the spider plots), whereas the fluorescence decrease ratio Rfd exhibited a significant decline in low light (shaded sectors of the spider graphs).

The spider plots in Fig. 2 can be considered as fluorescence fingerprints of the stress-induced changes in the photosynthetic processes induced by the individual treatments. The similarity of all three fluorescence fingerprints points to identical molecular mechanisms occurring with different dynamics upon infection of *A. thaliana* by virulent and avirulent strains of *P. syringae* and upon infiltration of leaf tissue with OPDA.

The effects of infiltration by jasmonic acid and salicylic acid were also investigated, but no change in the measured parameters exceeded noise. This observation indicates that there were no effects on fluorescence emission, or that the effects were too transient to be captured, or that the effects were systemic rather than localized.

Combinatorial fluorescence imaging

The selection of 19 parameters showing a fluorescence fingerprint (Fig. 2) represents those described earlier in the fluorescence literature (reviewed in Rohacek, 2002). These are typically used as standard parameters for the evaluation of chlorophyll fluorescence data. However, these are not necessarily the parameters that would yield the highest contrast between treated and untreated leaf tissue.

The problem of optimal selection of contrast-yielding fluorescence images is addressed in Matous *et al*. (2006). Here, a complex experimental protocol was applied with 331 independent fluorescence images capturing Kautsky induction and quenching analysis in 50 and 200 μmol m^{-2} s^{-1} and six transients in fluctuating, harmonically forced light (T=1.5, 3, 6, 12, 24, and 48 s) with two amplitudes 80 and 160 μmol m^{-2} s^{-1} (Supplementary data available at *JXB* online). By considering the complete set of fluorescence images and by Sequentional Forward Floating Search (Pudil *et al*., 1994), one can identify eight fluorescence images that yield the highest contrast between the infected and healthy leaf tissue (Supplementary data available at *JXB* online). The search can be trained using leaf tissue in the late phase of the infection (by the 24 h trained Late classifier) and, separately, using leaves in the early infection phase (6 h and 9 h trained Early classifier). Figure 3 shows how the algorithm classified individual pixels in fluorescence images of *A. thaliana* infected by the virulent strain (top block of Fig. 3, left) and the avirulent strain of *P. syringae* (top block of Fig. 3, right). The bottom figure block shows the classification for infiltration with OPDA (Fig. 3, bottom left) and with jasmonic acid (Fig. 3, bottom right). White shading indicates that the pixel was classified with confidence as belonging to the tissue in the early (left column) or late (right column) phase of the infection by the virulent strain. Black shading indicates that the pixel was classified as healthy tissue.

Figure 3 shows convincingly that the resolving power of the combinatorial fluorescence imaging significantly exceeds that of conventional fluorescence parameters in Figs 1 and 2. The classifier trained with leaves that were infected by the virulent strain of *P. syringae* for 6 h and 9 h was able to identify the infected tissue as early as 6 h after the infection by both virulent and avirulent strains. The symptoms were stronger in the avirulent strain than in the virulent strain. With advancing infection, the Early classifier faded away from the centre to the edge of the infected segment, indicating the early phase of the infection at the forefront. The Late classifier trained with leaves that were infected by the virulent strain of *P. syringae* for 24 h failed to recognize the early infection phase, while it was very powerful 24 h and 48 h after inoculation.

The fact that the classifiers trained with the virulent strain succeeded in recognizing correctly the infection by the avirulent strain confirms the earlier conclusion. The fluorescence signatures and thus the underlying effects on biochemical and/or molecular-genetic processes involved in photosynthesis are identical for both strains (Figs 2, 3).

Figure 3 also shows that the classifiers trained with the virulent strain of *P. syringae* can detect the effects of OPDA (left bottom) too. This proves that the signature is similar. The fluorescence signature of the infection was found sharply 3 h after the OPDA infiltration by the Late classifier and was only slightly weaker when identified by the Early classifier. The signature disappeared rapidly with only faint residues 24 h after the infiltration.

The combinatorial imaging failed to detect any symptoms when the leaf was infiltrated by jasmonic acid

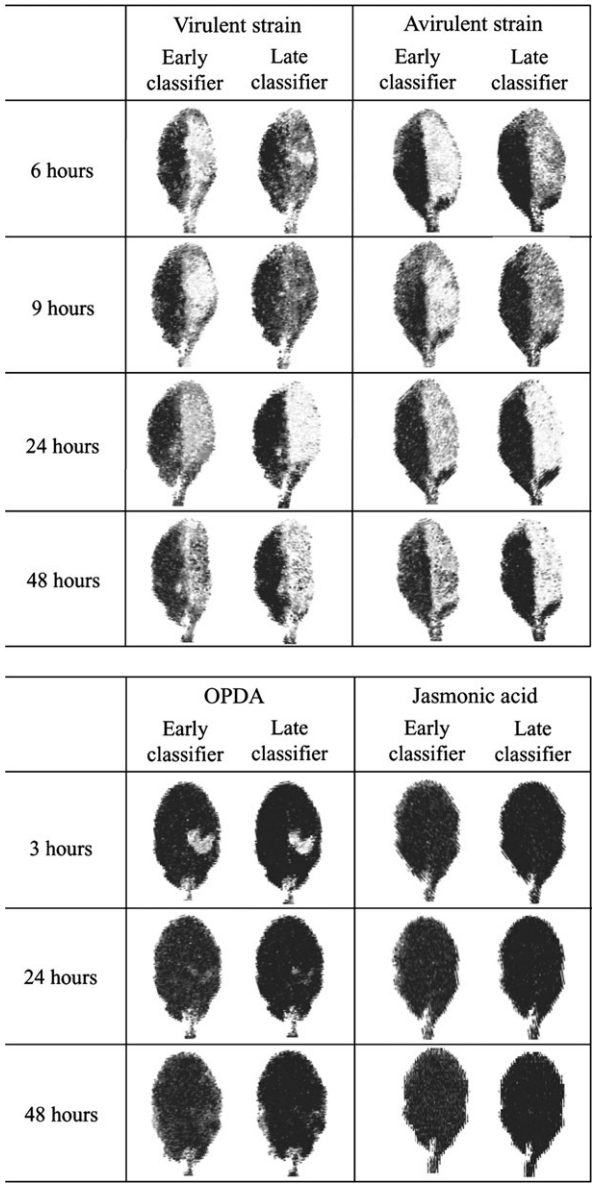

Fig. 3. The images generated by classification of individual pixels for their relative resemblance to fluorescence transients affected by 9 h (Early classifier) and by 24 h (Late classifier) of infection by the virulent strain of *P. syringae*. The white, non-shaded pixels emit fluorescence similar to the infected tissue, while the transients in black-shaded pixels are more similar to the healthy tissue. The classified fluorescence signals were limited to the eight most contrasting images identified by Sequentional Forward Floating Search in the fluorescence transient measured with the virulent strain. The shading scale was calculated as the ratio of Euclidian distance (Supplementary data available at *JXB* online) between the fluorescence signal in the particular pixel and the mean of its five nearest neighbours from the infected leaf segment and from the control leaf segment. The top left panel represents the classification trained with the selected image sets captured 9 h and 24 h, respectively, after infection by the virulent strain applied to the leaves attacked by the same strain. The top right panel shows classification trained with the virulent strain applied to the avirulent strain. The bottom panels show classification trained with the virulent strain applied to leaves infiltrated with OPDA (left) and with jasmonic acid (right).

(bottom right) and salicylic acid (not shown). This finding excludes one of the alternative explanations suggested above—a systemic response to the applied plant hormone would be detected as an 'all white' image in Fig. 3.

Discussion

Chlorophyll fluorescence imaging allows monitoring of the spatial distribution of photosynthetic activity and capacity. In addition, this non-invasive method provides the opportunity to measure temporal changes and kinetics of processes affecting photosynthetic performance. In this study, the method was applied to detect biotic stress responses and to analyse changes in photosynthesis in the interaction of the model organism *A. thaliana* with a virulent and an avirulent strain of *P. syringae*. Additionally, the changes upon pathogen infection were compared with the effect of the signalling molecules jasmonic acid, OPDA, and salicylic acid.

Kinetic chlorophyll fluorescence imaging is a well-established tool to image localized plant stress (reviewed in Nedbal and Whitmarsh, 2004). The investigated plant is dark-adapted, and the Kautsky-type fluorescence transient is elicited by sudden exposure to constant light and measured together with quenching analysis by saturating light flashes (Schreiber *et al*., 1986). Frequently, fluorescence parameters used conventionally in plant physiology are scanned and the one yielding the best contrast is used to detect the localized stress (Balachandran *et al*., 1997; Nedbal *et al*., 2000; Chaerle and Van der Straeten, 2001; Meyer *et al*., 2001; Soukupova *et al*., 2003; Berger *et al*., 2004; Chaerle *et al*., 2004). Here, a different strategy was used. A complex protocol was applied including Kautsky-type induction with two different irradiance levels and measurement of fluorescence dynamics in fluctuating, harmonically modulated light of various periods and amplitudes. The protocol is described in the Supplementary data available at *JXB* online. From this measurement, the conventional fluorescence parameters (Figs 1, 2) as well as 331 independent images were obtained. These images were submitted to a Sequentional Forward Floating Search (Pudil *et al*., 1994) for eight images that in combination yielded the highest contrast between the healthy tissue and tissue infected by the virulent strain of *P. syringae*. This combinatorial fluorescence imaging was shown to detect the infection as early as 6 h after the inoculation (Fig. 3), and the results indicate an even earlier detection (unpublished data). The technique also discriminated between the early and the late phases of the infection (Fig. 3).

The non-biased type of analysis to investigate and predict effects on photosynthesis by combinatorial fluorescence imaging (Fig. 3) was shown to be superior to the conventional approaches (Figs 1, 2) in identifying leaf

segments that are affected by the infection, as well as in its capacity to discriminate between the early and late phase of the infection. In contrast, imaging of the conventional fluorescence parameters has the great advantage of physiological interpretation. The F_V/F_M images shown in Fig. 1 reveal the effects of the infection only very late, after 24 h, but their interpretation provides a valuable insight: the capacity of PSII was locally reduced by the infection.

Photosynthesis decreased after treatment with both *P. syringae* strains. A decrease in photosynthesis, measured mostly as effective PSII quantum yield, has also been reported upon infection by biotrophic as well as necrotrophic pathogens in different plant systems (Balachandran *et al*., 1997; Nedbal *et al*., 2000; Chaerle and Van der Straeten, 2001; Meyer *et al*., 2001; Soukupova *et al*., 2003; Berger *et al*., 2004; Chaerle *et al*., 2004). This comprises compatible as well as incompatible interactions. In contrast, NPQ has been shown to be positively and negatively affected by pathogen attack. The effect on NPQ might depend on the amount of tissue damage. In tissue not heavily damaged, NPQ might increase based on stimulated electron flow as a protection mechanism (Schreiber, 2004). On the other hand, in severely damaged tissue, inhibition of photosynthetic electron transport might result in decreased NPQ.

Treatment with OPDA, but interestingly not with jasmonic acid or salicylic acid, resulted in a decrease in photosynthesis. OPDA is a reactive molecule, since it contains an α,β-unsaturated carbonyl structure (Almeras *et al*., 2003) while jasmonic acid and salicylic acid do not. This difference could explain why OPDA but not jasmonic acid or salicylic acid affected photosynthesis. It has been shown previously that different sugars, which can function as signalling molecules, decrease effective PSII quantum yield (Sinha and Roitsch, 2001). The present study demonstrates that the plant-derived lipid signalling molecule OPDA also exerts similar effects on chlorophyll fluorescence. Comparison of the fluorescence signature after treatment with both *P. syringae* strains and with OPDA revealed similarities of OPDA treatment 3 h after infiltration with *P. syringae* treatment 24 h and 48 h after infiltration. This observation is in agreement with an accumulation of OPDA 24 h after *P. syringae* infection (Block *et al*., 2005) and leads to the conclusion that OPDA might be involved in the down-regulation of photosynthesis caused by *P. syringae*. The fast decrease in F_V/F_M in response to OPDA infiltration indicates a direct effect of OPDA on PSII due to its reactivity (see above). The effects of OPDA treatment were transient, which might be due to diffusion and/or metabolism of the oxylipin. It is possible that within a few hours OPDA is converted to jasmonic acid, which is not active in changing photosynthetic parameters. Changes in photosynthesis were detectable earlier with the avirulent strain which induced stronger responses at the 6 h time point compared with the virulent strain. This is in agreement with the earlier detection of and defence induction against the avirulent strain (Dong *et al*., 1991; Baker *et al*., 1997).

The non-invasive analysis of plant primary metabolism by chlorophyll fluorescence imaging has particularly enriched stress physiological studies. The combination with other non-invasive techniques such as imaging of spontaneous photon emission (Bennett *et al*., 2005), and the detection of fluorescence reporter genes, labelled pathogens, and secondary metabolites should further upgrade the informative value of the approach. The present study demonstrates that both improvement of measurement protocols and optimization of the image analysis are important targets to be able to define fluorescence signatures that eventually allow discrimination between abiotic stress types and different pathogens. This will also be a prerequisite for online measurement in agricultural application for automation of fertilization and pest control.

Supplementary data

Numerical values of fluorescence parameters as well as a description of combinatorial imaging, complex actinic light protocols, and Euclidian distance are provided as Supplementary data associated with this article and are available at *JXB* online.

Acknowledgements

This work was supported in part by the Czech Ministry of Education, Sports, and Youth under the Grant MSM6007665808, by the Czech Academy of Sciences Grant AV0Z60870520, by the Grant Agency of the Czech Republic GACR 206/05/0894, and by the co-operative grants DAAD/CAS D28-CZ31/04-05 (TR) and the SFB 567 (SB). We are grateful to Sigrid Lux for her excellent technical assistance.

References

Almeras E, Stolz S, Vollenweider S, Reymond P, Mene-Saffrane L, Farmer EE. 2003. Reactive electrophile species activate defense gene expression in Arabidopsis. *The Plant Journal* **34,** 202–216.

Angrasharma R, Mandahar CL. 1993. Involvement of carbohydrates and cytokinins in pathogenicity of *Helminthosporium carbonum*. *Mycopathologia* **121,** 91–99.

Baker B, Zambryski P, Staskawicz B, DineshKumar SP. 1997. Signaling in plant–microbe interactions. *Science* **276,** 726–733.

Balachandran S, Hurry VM, Kelley SE, Osmond CB, Robinson SA, Rohozinski J, Seaton GGR, Sims DA. 1997. Concepts of plant biotic stress. Some insights into the stress physiology of virus-infected plants, from the perspective of photosynthesis. *Physiologia Plantarum* **100,** 203–213.

Balachandran S, Osmond CB, Daley PF. 1994. Diagnosis of the earliest strain-specific interactions between tobacco mosaic-virus

and chloroplasts of tobacco-leaves *in vivo* by means of chlorophyll fluorescence imaging. *Plant Physiology* **104,** 1059–1065.

Bennett M, Mehta M, Grant M. 2005. Biophoton imaging: a nondestructive method for assaying R gene responses. *Molecular Plant–Microbe Interaction* **18,** 95–102.

Berger S. 2002. Jasmonate-related mutants of Arabidopsis as tools for studying stress signaling. *Planta* **214,** 497–504.

Berger S, Papadopoulos M, Schreiber U, Kaiser W, Roitsch T. 2004. Complex regulation of gene expression, photosynthesis and sugar levels by pathogen infection in tomato. *Physiologia Plantarum* **122,** 419–428.

Block A, Schmelz E, Jones JB, Klee HJ. 2005. Coronatine and salicylic acid: the battle between *Arabidopsis* and *Pseudomonas* for phytohormone control. *Molecular Plant Pathology* **6,** 79–83.

Bonfig K, Schreiber U, Gabler A, Roitsch T, Berger S. 2006. Infection with virulent and avirulent *P. syringae* strains differentially affects photosynthesis and sink metabolism in Arabidopsis leaves. *Planta* (in press).

Buffoni M, Testi MG, Pesaresi P, Garlaschi FM, Jennings RC. 1998. A study of the relation between CP29 phosphorylation, zeaxanthin content and fluorescence quenching parameters in *Zea mays* leaves. *Physiologia Plantarum* **102,** 318–324.

Chaerle L, Hagenbeek D, De Bruyne E, Valcke R, Van der Straeten D. 2004. Thermal and chlorophyll-fluorescence imaging distinguish plant–pathogen interactions at an early stage. *Plant and Cell Physiology* **45,** 887–896.

Chaerle L, Van der Straeten D. 2001. Seeing is believing: imaging techniques to monitor plant health. *Biochimica et Biophysica Acta* **1519,** 153–166.

Creelman RA, Mullet JE. 1997. Biosynthesis and action of jasmonates in plants. *Annual Review of Plant Physiology and Plant Molecular Biology* **48,** 355–381.

Cui J, Bahrami AK, Pringle EG, Hernandez-Guzman G, Bender CL, Pierce NE, Ausubel FM. 2005. *Pseudomonas syringae* manipulates systemic plant defenses against pathogens and herbivores. *Proceedings of the National Academy of Sciences, USA* **102,** 1791–1796.

Dangl JL, Jones JDG. 2001. Plant pathogens and integrated defence responses to infection. *Nature* **411,** 826–833.

Delaney TP, Uknes S, Vernooij B, *et al*. 1994. A central role of salicylic acid in plant disease resistance. *Science* **266,** 1247–1250.

Devoto A, Turner JG. 2005. Jasmonate-regulated Arabidopsis stress signalling network. *Physiologia Plantarum* **123,** 161–172.

Dong XN, Mindrinos M, Davis KR, Ausubel FM. 1991. Induction of Arabidopsis defense genes by virulent and avirulent *Pseudomonas syringae* strains and by a cloned avirulence gene. *The Plant Cell* **3,** 61–72.

Ehness R, Ecker M, Godt DE, Roitsch T. 1997. Glucose and stress independently regulate source and sink metabolism and defense mechanisms via signal transduction pathways involving protein phosphorylation. *The Plant Cell* **9,** 1825–1841.

Genty B, Briantais J-M, Baker NR. 1989. The relationship between quantum yield of photosynthetic electron transport and quenching of chlorophyll fluorescence. *Biochimica et Biophysica Acta* **990,** 87–92.

Heath MC. 2000. Hypersensitive response-related death. *Plant Molecular Biology* **44,** 321–334.

Herbers K, Meuwly P, Frommer WB, Metraux JP, Sonnewald U. 1996. Systemic acquired resistance mediated by the ectopic expression of invertase: possible hexose sensing in the secretory pathway. *The Plant Cell* **8,** 793–803.

Horton P, Ruban AV. 1992. Regulation of photosystem-II. *Photosynthesis Research* **34,** 375–385.

Jang JC, Sheen J. 1994. Sugar sensing in higher-plants. *The Plant Cell* **6,** 1665–1679.

Lichtenthaler HK, Babani F. 2000. Detection of photosynthetic activity and water stress by imaging the red chlorophyll fluorescence. *Plant Physiology and Biochemistry* **38,** 889–895.

Lichtenthaler HK, Buschmann C, Knapp M. 2005*a*. How to correctly determine the different chlorophyll fluorescence parameters and the chlorophyll fluorescence decrease ratio R–Fd of leaves with the PAM fluorometer. *Photosynthetica* **43,** 379–393.

Lichtenthaler HK, Langsdorf G, Lenk S, Buschmann C. 2005*b*. Chlorophyll fluorescence imaging of photosynthetic activity with the flash-lamp fluorescence imaging system. *Photosynthetica* **43,** 355–369.

Lichtenthaler HK, Miehe JA. 1997. Fluorescence imaging as a diagnostic tool for plant stress. *Trends in Plant Science* **2,** 316–320.

Matous K, Benediktyova Z, Berger S, Roitsch T, Nedbal L. 2006. Case study of combinatorial imaging: what protocol and what chlorophyll fluorescence image to use when visualizing infection of *Arabidopsis thaliana* by *Pseudomonas syringae*? *Photosynthesis Research* (in press).

Maxwell K, Johnson GN. 2000. Chlorophyll fluorescence: a practical guide. *Journal of Experimental Botany* **51,** 659–668.

Meyer S, Saccardy-Adji K, Rizza F, Genty B. 2001. Inhibition of photosynthesis by *Colletotrichum lindemuthianum* in bean leaves determined by chlorophyll fluorescence imaging. *Plant, Cell and Environment* **24,** 947–955.

Mur LAJ, Kenton P, Atzorn R, Miersch O, Wasternack C. 2006. The outcomes of concentration-specific interactions between salicylate and jasmonate signaling include synergy, antagonism, and oxidative stress leading to cell death. *Plant Physiology* **140,** 249–262.

Nedbal L, Brezina V. 2002. Complex metabolic oscillations in plants forced by harmonic irradiance. *Biophysical Journal* **83,** 2180–2189.

Nedbal L, Brezina V, Adamec F, Stys D, Oja V, Laisk A, Govindjee. 2003. Negative feedback regulation is responsible for the non-linear modulation of photosynthetic activity in plants dynamic light and cyanobacteria exposed to a environment. *Biochimica et Biophysica Acta* **1607,** 5–17.

Nedbal L, Brezina V, Cerveny J, Trtilek M. 2005. Photosynthesis in dynamic light: systems biology of unconventional chlorophyll fluorescence transients in *Synechocystis* sp. PCC 6803. *Photosynthesis Research* **84,** 99–106.

Nedbal L, Soukupova J, Whitmarsh J, Trtilek M. 2000. Postharvest imaging of chlorophyll fluorescence from lemons can be used to predict fruit quality. *Photosynthetica* **38,** 571–579.

Nedbal L, Whitmarsh J. 2004. Chlorophyll fluorescence imaging of leaves and fruits. In: Papageorgiu G, Govindjee, eds. *Chlorophyll a fluorescence: a signature of photosynthesis*. Dordrecht, The Netherlands: Springer, 389–407.

Oxborough K. 2004. Imaging of chlorophyll *a* fluorescence: theoretical and practical aspects of an emerging technique for the monitoring of photosynthetic performance. *Journal of Experimental Botany* **55,** 1195–1205.

Parchmann S, Gundlach H, Mueller MJ. 1997. Induction of 12-oxo-phytodienoic acid in wounded plants and elicited plant cell cultures. *Plant Physiology* **115,** 1057–1064.

Pudil P, Novovicova J, Kittler J. 1994. Floating search methods in feature selection. *Pattern Recognition Letters* **15,** 1119–1125.

Raacke IC, Mueller MJ, Berger S. 2006. Defects in allene oxide synthase and OPDA reductase alter the resistance to *Pseudomonas syringae* and *Botrytis cinerea*. *Journal of Phytopathology* (in press).

Rohacek K. 2002. Chlorophyll fluorescence parameters: the definitions, photosynthetic meaning, and mutual relationships. *Photosynthetica* **40,** 13–29.

Roitsch T, Balibrea ME, Hofmann M, Proels R, Sinha AK. 2003. Extracellular invertase: key metabolic enzyme and PR protein. *Journal of Experimental Botany* **54,** 513–524.

Roitsch T, Gonzalez MC. 2004. Function and regulation of plant invertases: sweet sensations. *Trends in Plant Science* **9,** 606–613.

Scharte J, Schon H, Weis E. 2005. Photosynthesis and carbohydrate metabolism in tobacco leaves during an incompatible interaction with *Phytophthora nicotianae*. *Plant, Cell and Environment* **28,** 1421–1435.

Scholes JD, Rolfe SA. 1996. Photosynthesis in localised regions of oat leaves infected with crown rust (*Puccinia coronata*): quantitative imaging of chlorophyll fluorescence. *Planta* **199,** 573–582.

Schreiber U. 2004. Pulse-amplitude-modulation (PAM) fluorometry and saturation pulse method: an overview. In: Papageorgiu G, Govindjee, eds. *Chlorophyll* a *fluorescence. A signature of photosynthesis*. Dordrecht, The Netherlands: Springer, 279–319.

Schreiber U, Schliwa U, Bilger W. 1986. Continuous recording of photochemical and non-photochemical chlorophyll fluorescence quenching with a new type of modulation fluorometer. *Photosynthesis Research* **10,** 51–62.

Sinha AK, Hofmann MG, Romer U, Kockenberger W, Elling L, Roitsch T. 2002. Metabolizable and non-metabolizable sugars activate different signal transduction pathways in tomato. *Plant Physiology* **128,** 1480–1489.

Sinha AK, Roitsch T. 2001. Effect of different sugars on photosynthesis and chlorophyll fluorescence in photoautotrophic tomato suspension cell cultures. *Photosynthetica* **39,** 611–614.

Soukupova J, Smatanova S, Nedbal L, Jegorov A. 2003. Plant response to destruxins visualized by imaging of chlorophyll fluorescence. *Physiologia Plantarum* **118,** 399–405.

Stintzi A, Weber H, Reymond P, Browse J, Farmer EE. 2001. Plant defense in the absence of jasmonic acid: the role of cyclopentenones. *Proceedings of the National Academy of Sciences, USA* **98,** 12837–12842.

Taki N, Sasaki-Sekimoto Y, Obayashi T, *et al*. 2005. 12-Oxo-phytodienoic acid triggers expression of a distinct set of genes and plays a role in wound-induced gene expression in Arabidopsis. *Plant Physiology* **139,** 1268–1283.

Tao Y, Xie ZY, Chen WQ, Glazebrook J, Chang HS, Han B, Zhu T, Zou GZ, Katagiri F. 2003. Quantitative nature of Arabidopsis responses during compatible and incompatible interactions with the bacterial pathogen *Pseudomonas syringae*. *The Plant Cell* **15,** 317–330.

van Kooten O, Snel JFH. 1990. The use of chlorophyll fluorescence nomenclature in plant stress physiology. *Photosynthesis Research* **25,** 147–150.